© 2019. Published by The Company of Biologists Ltd | Journal of Experimental Biology (2019) 222, jeb191197. doi:10.1242/jeb.191197

RESEARCH ARTICLE

Do naked mole rats accumulate a metabolic acidosis or an oxygen debt in severe hypoxia?

Matthew E. Pamenter[1,2,3,*,‡], Yvonne A. Dzal[3,4,*], William A. Thompson[3,5] and William K. Milsom[3]

ABSTRACT

In severe hypoxia, most vertebrates increase anaerobic energy production, which results in the development of a metabolic acidosis and an O_2 debt that must be repaid during reoxygenation. Naked mole rats (NMRs) are among the most hypoxia-tolerant mammals, capable of drastically reducing their metabolic rate in acute hypoxia while staying active and alert. We hypothesized that a key component of remaining active is an increased reliance on anaerobic metabolism during severe hypoxia. To test this hypothesis, we exposed NMRs to progressive reductions in inspired O_2 (9–3% O_2) followed by reoxygenation (21% O_2) and measured breathing frequency, heart rate, behavioural activity, body temperature, metabolic rate, and also metabolic substrates and pH in blood and tissues. We found that NMRs exhibit robust metabolic rate depression in acute hypoxia, accompanied by declines in all physiological and behavioural variables examined. However, blood and tissue pH were unchanged, and tissue concentrations of ATP and phosphocreatine were maintained. NMRs increased their reliance on carbohydrates in hypoxia, and glucose was mobilized from the liver to the blood. Upon reoxygenation, NMRs entered into a coma-like state for ∼15–20 min, during which metabolic rate was negligible and body temperature remained suppressed. However, an imbalance in the time taken for the rates of O_2 uptake ($\dot{V}_{O_2}$) and CO_2 production ($\dot{V}_{CO_2}$) to return to normoxic levels during reoxygenation hint at the possibility that NMRs do utilize anaerobic metabolism during hypoxia but have a tissue and/or blood buffering capacity that masks typical markers of metabolic acidosis, and that the synthesis of glucose from lactate, rather than lactate oxidation, is prioritized during recovery.

KEY WORDS: Hypoxic metabolic response, Hypoxic ventilatory response, Anaerobic metabolism, Thermoregulation, Behaviour, Metabolic fuel switching

INTRODUCTION

Although mammals are largely intolerant of hypoxia, a few species inhabit hypoxic niches (e.g. some fossorial species and species resident to high altitudes). These animals have evolved complicated suites of physiological and molecular adaptations that enable them to thrive in low O_2 environments (Dzal et al., 2015). The key to tolerating prolonged hypoxia is to match metabolic demand to reduced energy (O_2) supply (Buck and Pamenter, 2006, 2018; Hochachka, 1986; Hochachka et al., 1996), with most hypoxia-tolerant animals exhibiting robust decreases in metabolic rate when O_2 supplies are limited (Dzal et al., 2015; Guppy and Withers, 1999). Conversely, hypoxia-intolerant animals are generally unable to sufficiently reduce their metabolic rate during hypoxia to accommodate the reduced O_2 supply and instead increase ventilation in a largely futile attempt to maintain O_2 supply. This is an energetically expensive strategy, particularly when breathing air with reduced O_2 content (Dzal et al., 2015; Pamenter and Powell, 2016). As a result, and in the absence of sufficient metabolic rate depression in severe hypoxia, most mammals rely on anaerobic energy production to make up the gap between energy demand and their ability to produce energy aerobically (Buck and Pamenter, 2006; Hochachka, 1986).

Anaerobic metabolism (primarily glycolysis) usually leads to the accumulation of lactate and, upon reoxygenation, this accumulated lactate must either be oxidized to CO_2 and H_2O via the tricarboxylic acid cycle, converted to glucose/glycogen via gluconeogenesis in the liver and/or muscle, or utilized in protein synthesis (Warren and Jackson, 2008). Oxidation is the predominate end-point for lactate that accumulates during hypoxia in most mammals and it yields 15 molecules of ATP per molecule of lactate oxidized; however, this process also requires metabolic O_2. As a result, animals that utilize this pathway typically hyperventilate and exhibit a high rate of O_2 consumption ($\dot{V}_{O_2}$) during reoxygenation, reflecting repayment of the O_2 debt accrued during hypoxic exposure (Robin, 1980). This phenomenon has been observed in both individual organs and whole animals across a wide range of adult vertebrate species following exposure to hypoxia (Coffman, 1963; Lewis et al., 2007; Maxime et al., 2000; Plambech et al., 2013; Svendsen et al., 2012). In all of these species, the elevated metabolic rate upon reoxygenation correlates with the level of metabolic acidosis and elevated lactate concentration in the blood and/or tissues. Little is known regarding lactate accumulation and clearance in hypoxia-tolerant mammals, but animals that are capable of robust metabolic rate depression during acute hypoxia typically do not exhibit an O_2 debt upon reoxygenation, and lactate accumulation is minimal (Frappell et al., 1991). For example, in hypoxia-tolerant neonatal mammals, instead of metabolic rate overshooting baseline levels during reoxygenation from hypoxia (15% O_2), $\dot{V}_{O_2}$ quickly returns to pre-hypoxic levels and lactate accumulation is only observed in more severe hypoxia (10% O_2) (Frappell et al., 1991).

Naked mole rats (NMRs; *Heterocephalus glaber* Rüppell 1842) are the most hypoxia-tolerant mammal presently identified and tolerate minutes of anoxia, hours at 3% O_2 and days to weeks at 8% O_2 (Chung et al., 2016; Pamenter et al., 2015, 2018; Park et al., 2017). In acute severe hypoxia (3% O_2), the $\dot{V}_{O_2}$ of adult NMRs decreases up to 85% (Pamenter et al., 2018). Although this degree of $\dot{V}_{O_2}$ suppression is not remarkable among hypoxia-tolerant species

[1]Department of Biology, University of Ottawa, Ottawa, ON, Canada, K1S 9N3. [2]University of Ottawa Brain and Mind Research Institute, Ottawa, ON, Canada. [3]Department of Zoology, University of British Columbia, Vancouver, BC, Canada, V6T 1Z4. [4]Department of Biology and Centre for Forest Interdisciplinary Research, University of Winnipeg, Winnipeg, MB, Canada, R3B 2E9. [5]Department of Biology, University of Calgary, Calgary, AB, Canada, T2N 1N4.
*These authors contributed equally to this work

‡Author for correspondence (mpamenter@uottawa.ca)

M.E.P., 0000-0003-4035-9555; W.K.M., 0000-0002-0866-7489

Received 23 August 2018; Accepted 18 December 2018

(Guppy and Withers, 1999), it is important to note that other adult mammals that are capable of similar or more extreme metabolic rate suppression in severe hypoxia typically enter into a coma- or torpor-like state until O_2 levels increase (Guppy and Withers, 1999; Hayden and Lindberg, 1970). Conversely, NMRs remain awake and active (albeit to a reduced degree) in hypoxia (Houlahan et al., 2018; Ilacqua et al., 2017; Kirby et al., 2018). This combined metabolic and behavioural phenotype (robust metabolic rate depression combined with the retained ability to ambulate and interact within their environment) may be a unique characteristic of this remarkable species. Unfortunately, previous studies have not evaluated the physiological and biochemical mechanisms that support the NMR's remarkable ability to stay active in severe hypoxia, leaving an important question unanswered: do NMRs employ anaerobic metabolism to support behavioural activity during metabolic suppression?

In the present study, we comprehensively evaluated physiological and behavioural variables in NMRs across a wide range of hypoxic exposures and also during reoxygenation. We hypothesized that NMRs rely on anaerobic metabolism during hypoxia and thus would exhibit signs of an accumulated O_2 debt after hypoxia. We predicted that they would exhibit a metabolic acidosis and a deficit in energetic substrate pools (e.g. ATP) during hypoxia, and an overshoot in $\dot{V}_{O_2}$ during reoxygenation. To test our hypothesis, we exposed NMRs to progressive hypoxia (21–3% O_2), followed by a 1 h reoxygenation period, and measured breathing and heart rates (i.e. the primary components of O_2 supply), behavioural activity, body temperature (T_b) and metabolism (i.e. the primary consumers of O_2) throughout these exposures. Additionally, at the end of the hypoxic protocol, a subset of animals were euthanized to collect blood and tissues from which we analyzed markers indicative of metabolic acidosis and energy balance.

MATERIALS AND METHODS

Animals

NMRs were group-housed in interconnected multi-cage systems at 30°C and 21% O_2 in 50% relative humidity with a 12 h:12 h light: dark cycle. Animals were fed fresh tubers, vegetables, fruit, and Pronutro cereal supplement *ad libitum*. Animals were not fasted prior to experimental trials. All experimental procedures were approved by the University of British Columbia Animal Care Committee (Protocol A13-0248) in accordance with the Animals for Research Act and by the Canadian Council on Animal Care. All experiments were performed during daylight working hours in the middle of the animals' 12 h:12 h light:dark cycle. NMRs that are housed within colony systems, as our experimental animals are, do not exhibit circadian rhythmicity of general locomotor activity (Riccio and Goldman, 2000b) and exhibit inconsistent rhythmicity of T_b and metabolic rate (Riccio and Goldman, 2000a); however, significant changes in these latter variables were only reported in animals during the nocturnal phase of their circadian cycle, with no significant changes observed during the daylight period of this cycle. Therefore, since we only ran experimental trials during the daylight period, we did not expect our results to be influenced by circadian rhythms. We examined physiological responses to environmental hypoxia in non-breeding NMRs that were 1–2 years old. Non-breeding (subordinate) NMRs do not undergo sexual development or express sexual hormones and thus we did not take sex into consideration when evaluating our results (Holmes et al., 2009).

Whole-body plethysmography and respirometry

Twenty-two adult, non-breeding male and female NMRs, weighing 39.0±4.6 g (mean±s.e.m.) were individually placed, unrestrained, inside a 450 ml Plexiglass experimental chamber (the animal chamber), which was in turn placed into an environmental chamber held at ∼28–29°C. The temperature of the animal chamber was recorded continuously throughout the experiment using multiple iButtons that recorded ambient temperature (T_a) at a frequency of one measurement min^{-1} (Maxim Integrate, Chandler, QC, Canada). Animals were provided with a thin layer of bedding on the floor of the experimental chambers. The animal chamber was sealed and constantly ventilated with gas mixtures, set to the desired fractional gas composition by calibrated rotameters (Praxair, Mississauga, ON, Canada). The advantage of this open-flow system is that it prevents the depletion of O_2 and accumulation of metabolic CO_2 by flushing the animal chamber with fresh gas, and it allows for continuous and simultaneous monitoring of metabolic and ventilatory variables. Inflowing gas was provided at a flow rate of 110 ml min^{-1}, as assessed by a calibrated mass flow meter (Praxair Technologies Inc., Danbury, CT, USA). The analyzers were calibrated prior to each trial with 20.95% O_2 and 1.5% CO_2, both balanced with N_2, and with 100% N_2 gas mixtures. During experimentation, animal ventilation caused pressure fluctuations due to humidity and the warmth of air in each expired breath, which were compared to the pressure of a reference chamber that was identical to the animal chamber. Continuous monitoring by a differential pressure transducer (Validyne, Northridge, CA, USA) connected between the animal and reference chambers allowed for the detection of breaths. Breathing frequency (f_R) was determined by counting these ventilation-induced pressure oscillations. All ventilatory variables are reported at body temperature, pressure, saturated (BTPS).

$\dot{V}_{O_2}$ and $\dot{V}_{CO_2}$ (CO_2 production rate) were measured by analyzing the outflowing composition of gas by a Sable Systems FC-10 O_2 analyzer and a Sable Systems CA-10 CO_2 analyzer, respectively, and comparing it to the inflow gas concentrations (Sable Systems, Las Vegas, NV, USA). $\dot{V}_{O_2}$ and $\dot{V}_{CO_2}$ were calculated using equations 10.6 and 10.7 in Lighton (2008), respectively:

$$\dot{V}_{O_2} = \dot{V}_i[(F_{I_{O_2}} - F_{E_{O_2}}) - F_{E_{O_2}}(F_{E_{CO_2}} - F_{I_{CO_2}})]/(1 - F_{E_{O_2}}), \quad (1)$$

$$\dot{V}_{CO_2} = \dot{V}_i[(F_{E_{CO_2}} - F_{I_{CO_2}}) - F_{E_{CO_2}}(F_{I_{O_2}} - F_{E_{O_2}})]/(1 - F_{E_{CO_2}}), \quad (2)$$

where $\dot{V}_{O_2}$ is the O_2 consumption rate (ml min^{-1}) and $\dot{V}_{CO_2}$ is the CO_2 production rate (ml min^{-1}), $\dot{V}_i$ is incurrent flow rate (ml min^{-1}), $F_{I_{O_2}}$ and $F_{I_{CO_2}}$ are fractional concentrations of incurrent O_2 and CO_2 of dry gas, respectively, and $F_{E_{O_2}}$ and $F_{E_{CO_2}}$ are fractional concentrations of excurrent O_2 and CO_2 of dry gas, respectively (Lighton, 2008). The respiratory exchange ratio (RER) was calculated by dividing $\dot{V}_{CO_2}$ by $\dot{V}_{O_2}$. All metabolic variables are reported at standard temperature and pressure, dry (STPD).

Pulse oximetry and blood parameters

Heart rate, arterial O_2 saturation (S_{a,O_2}) and behavioural activity (active/inactive) were also measured *in vivo* using pulse oximetry collars (STARR Life Sciences Corp., Oakmont, PA, USA). Blood pH (pH_a), partial pressure of CO_2 (P_{CO_2}; mmHg), partial pressure of O_2 (P_{O_2}; mmHg), base excess, [HCO_3^-] (mmol l^{-1}), total CO_2 in the blood (T_{CO_2}, which includes free CO_2 in the plasma and bound to proteins, as well as in the form of bicarbonate, carbonic anions and carbonic acid), [Na^+] (mmol l^{-1}), [K^+] (mmol l^{-1}), intracellular [Ca^{2+}] ($[Ca^{2+}]_i$; mmol l^{-1}), [glucose] (mg dl^{-1}), haemoglobin

concentration ([Hb]; mmol l^{-1}) and haematocrit (Hct; %) were analyzed *ex vivo* from blood at 30°C (which is approximately the NMR T_b at our experimental T_a in hypoxia) using $CG8^+$ cartridges with the i-STAT VetScan Analyzer (Abaxis, Union City, CA, USA). Haematocrit was also calculated from the ratio of the volume of packed red blood cells to the total blood volume after centrifugation in micro-haematocrit tubes (~10 µl). Haemoglobin concentration was also determined by the cyanmethaemoglobin method using Drabkin's reagent (Sigma-Aldrich, St Louis, MO, USA) and a haem-based extinction coefficient of 11 $mmol^{-1}$ cm^{-1} at a wavelength of 540 nm.

Body temperature

In a separate experiment, T_b was measured from a group of eight NMRs held individually in cages at 28.4°C and 70% relative humidity and exposed to the same progressive hypoxia/reoxygenation treatment protocol as described above. In these experiments, T_b was measured using a handheld radio frequency identification (RFID) reader that scanned individual NMRs instrumented with subcutaneous RFID microchips (Destron Fearing, Dallas, TX) every 30 min, as described previously (Kirby et al., 2018). Measurements were taken when the body region containing the RFID microchip was not in contact with the floor to avoid skewed readings.

Experimental design

Animals were transferred to the animal chamber under normoxic conditions and baseline recordings were obtained for 1 h. The inflowing gas composition was then switched progressively to 9, 7, 5 and 3% O_2 for 1 h each. Finally, the inflowing gas concentration was switched back to 21% O_2 for 1 h. Following experimentation, animals were returned to their colonies. At the end of the hypoxic protocol, a subset of animals were euthanized by conscious cervical dislocation followed immediately by decapitation to assess blood and tissue parameters. Tissues were removed within 2 min of decapitation, snap-frozen in liquid nitrogen and then stored at −80°C for future analysis.

Intracellular pH and metabolite measurements

Frozen temporalis muscle, liver, heart and brain tissue were ground into a fine powder under liquid nitrogen using mortar and pestle. Tissues were aliquoted and used for intracellular pH (pH_i), creatine phosphate (CrP), ATP and glucose analysis. For pH_i, frozen tissue was mixed with a metabolic inhibitor solution [150 mmol l^{-1} KF; 6 mmol l^{-1} nitrilotriacetic acid (Sigma)] using a liquid-nitrogen-cooled 18-gauge needle, and vortexed. Samples were centrifuged at 10,000 ***g*** for 1 min, then the supernatant was removed and incubated at 30°C in a water bath for 15 min. Following the incubation period, pH_i was recorded using a calibrated semi-micro pH electrode (Cole-Parmer, IL). The pH probe was re-calibrated every four samples and held in a metabolic inhibitor solution between sample measurements.

Frozen tissue for CrP, ATP and glucose analysis was homogenized in 8% $HClO_3$ and stored on ice. Samples were neutralized with NaOH, and the supernatant was removed and aliquoted for either CrP and ATP, or glucose determination. CrP and ATP were determined using a modified technique from Bergmeyer (1965). A total of 100 µl of neutralized extract was mixed with 150 µl of assay buffer [7 ml buffered base solution (50 mmol l^{-1} Tris base; 8 mmol l^{-1} $MgCl_2{\cdot}6H_2O$; 50 mmol l^{-1} glucose; 2 mmol l^{-1} $EDTA{\cdot}Na_2{\cdot}H_2$; mercaptoethanol; adjusted to pH 8.0); 10 mg βNADP; 20 µl glucose 6-phosphate dehydrogenase (3520.3 U ml^{-1}); Sigma]. Samples were incubated at 37°C for 5 min and absorbance was recorded at 340 nm (A_1). Hexokinase (150 U ml^{-1}; Sigma) was added (2 µl), and samples were then incubated at room temperature for 15 min before recording absorbance (A_2). A total of 5 mmol l^{-1} adenosine diphosphate (ADP) (20 µl) was added, with samples left to incubate at room temperature for 5 min, and absorbance was measured (A_3). Finally, 2 µl of creatine kinase (10 mg ml^{-1}; Sigma) was added, and samples were incubated at room temperature for 20 min before recording absorbance (A_4). ATP was calculated as A_2–A_1 and CrP as A_4–A_3. Standards between 0–500 µmol l^{-1} and 0–2000 µmol l^{-1} were used for ATP and CrP, respectively.

Glucose was determined using 20 µl of neutralized sample and adding 100 µl of assay buffer [17 ml of 4 mmol l^{-1} $MgCl_2{\cdot}6H_2O$ 83 mmol l^{-1} NaH_2PO_4; 20.67 mg βNADP; 14.88 g ATP; 10 µl glucose 6-phosphate dehydrogenase (1.5 U ml^{-1})]. Samples were incubated for 5 min at 37°C and absorbance was read at 340 nm (A_1). Hexokinase (2 µl; 2.25 U ml^{-1}; Sigma) was added to each sample, which was incubated for 20 min at 37°C, and absorbance was recorded (A_2). Glucose was calculated as A_2–A_1 using a standard curve between 0–5 mmol l^{-1}. Adenylate energy charge was calculated using [CrP], [ATP] and pH_i measurements. Estimates of inorganic phosphate (Pi) were determined as the inverse of CrP hydrolysis, assuming a normoxic Pi concentration of approximately 1 µmol g^{-1} wet mass for each tissue (Portner et al., 1996). Assuming equilibrium of the creatine kinase and adenylate kinase reactions, and stoichiometry of creatine phosphate and Pi (Lawson and Veech, 1979), ADP and adenosine monophosphate (AMP) were estimated based on the formula described previously (Lanza et al., 2006). Equilibrium constants for creatine kinase and adenylate kinase were corrected for pH and temperature, while assuming a concentration of free Mg^{2+} of 0.001 mol l^{-1} (Golding et al., 1995; Teague et al., 1996). Adenylate free energy charge was calculated as described previously (Atkinson, 1968).

Data collection and statistical analysis

T_b, incurrent and excurrent O_2 and CO_2 concentrations, and the ventilation-induced pressure signals were recorded and analyzed using PowerLab data acquisition hardware and LabChart software (AD Instruments Ltd, Colorado Springs, CO, USA). Pulse oximetry data were recorded using MouseOx Plus (STARR Systems). From the recorded signals, and calculated dependent variables, we determined average T_b, $\dot{V}_{O_2}$, $\dot{V}_{CO_2}$, RER, f_R, S_{a,O_2}, heart rate and behavioural activity state for the last 10–15 min of each O_2 exposure (21, 9, 7, 5, 3% O_2), and for the last 1–2 min of each 10 min period of post-hypoxia recovery (10, 20, 30, 40, 50, 60 min reoxygenation). Inflowing gas concentrations were measured before and after each O_2 exposure. Upon reoxygenation, we were unable to measure $\dot{V}_{O_2}$ for ~20 min due to a combination of the volume of the animal chamber, the slow rate of gas flow through the animal chamber (and thus the long washout period), and the large difference between O_2 levels in the incurrent gases supplied during hypoxia and normoxia treatments (3 and 21%, respectively). Conversely, incurrent gas CO_2 levels did not differ between hypoxia and normoxia, and so we were able to measure $\dot{V}_{CO_2}$ during the early reoxygenation phase as an indirect measure of metabolic rate.

Statistical analyses were performed using R (http://www.R-project.org/) and GraphPad Prism 7.0. We used linear mixed effects models (lme4 and lsmeans package) (Bates et al., 2015; Lenth, 2016) to account for repeated sampling of the same individual with changes in O_2 exposure, with individual treated as a random effect. All physiological and behavioural variables met the assumptions of normality, homogeneity of variances, linearity and independence. We entered the level of inspired O_2 and body mass as fixed effects in

our models. We ran a Tukey's *post hoc* test using the lsmeans package to determine differences between inspired O_2 levels and to correct for multiple pairwise comparisons to test for differences between normoxia and hypoxia-treated samples. Blood and tissue data were analyzed using Student's *t*-tests. All results are presented as means±s.e.m., with statistical significance set as $P<0.05$.

RESULTS

Breathing frequency, heart rate and behavioural activity decreased with decreasing arterial blood saturation throughout progressive hypoxia

S_{a,O_2}, heart rate and behavioural activity were measured using a pulse oximeter. NMRs are very flexible and agile and, in most experiments, they were able to free themselves from the pulse oximeter collar or to bite through the electric lead. As a result, S_{a,O_2}, heart rate, and activity data are presented only for the subset of animals exposed to progressive hypoxia from which pulse oximeter data were obtained throughout the experiment (i.e. for each level of O_2). Arterial blood was fully saturated with O_2 in normoxia (21% O_2) and saturation significantly decreased with progressive hypoxia (Fig. 1A, left panel; $F_{4,35}=8.153$, $P<0.0001$; $n=8$). S_{a,O_2} decreased significantly to ∼90% when NMRs were breathing 9% O_2, further decreased to 60–70% when animals were breathing 7–5% O_2, and then dipped significantly to ∼40% saturation when NMRs were breathing 3% O_2. Upon reoxygenation, S_{a,O_2} rapidly returned to baseline levels (within 10 min) (Fig. 1A, right panel).

Breathing frequency decreased by ∼25% (from ∼90 breaths min^{-1} in normoxia) in 9% O_2 and then decreased further and plateaued at ∼60 breaths min^{-1} at inhaled O_2 levels ranging from 7 to 3% O_2 (Fig. 2B, left panel; $F_{10,116}=4.13$, $P<0.00001$; $n=22$). Upon reoxygenation (within 10 min), f_R decreased further to ∼50% of the normoxic breathing rate (Fig. 1B, right panel). Over the ensuing 50 min of reoxygenation, f_R continued to increase back to the pre-hypoxia baseline and was not statistically different from normoxic levels after 50 min of reoxygenation.

Heart rate significantly decreased in progressive hypoxia. When NMRs were breathing hypoxic gas containing 9 and 7% O_2, heart rate decreased by 17% from the normoxic levels of ∼220 beats min^{-1} (Fig. 1C, left panels; $n=8$), and then decreased by 30 and 40% of normoxic levels when animals were breathing 5 and 3% O_2, respectively ($F_{4,35}=13.65$, $P<0.0001$). Upon reoxygenation, heart rate did not fall further but increased more rapidly than f_R, such that heart rate was not different from pre-hypoxia normoxic levels after 30 min of reoxygenation (Fig. 1C, right panel).

Behavioural activity, as indicated by total time active min^{-1}, was not different at 9% O_2 relative to normoxic levels but decreased by ∼65% when animals were breathing 7–5% O_2 and by 85% of normoxic levels when animals were breathing 3% O_2 (Fig. 1D, left panel; $F_{4,35}=20.1$, $P<0.0001$; $n=8$). Following reoxygenation, NMRs appeared to enter into a fully comatose state for the first 15–20 min (Fig. 1D, right panel). Animals were completely motionless and, in a subset of experiments, we were compelled to open the chamber to check on the health of the animals. Animals were non-responsive to auditory, visual or mechanical stimuli. Breaths were difficult to detect visually. However, following ∼20–30 min of reoxygenation, all animals regained consciousness and ambulated normally.

Body temperature decreased to near ambient temperatures with progressive hypoxia

In normoxia, NMR T_b was ∼3–4°C above T_a (Fig. 2; $n=8$). With the onset of acute hypoxia, T_b decreased by ∼2°C at 9% O_2, and then progressively decreased by ∼0.5°C at each further level of progressive hypoxia, finally reaching a minimal level that was within 0.5°C of T_a in animals breathing 3% O_2 ($F_{7,63}=6.10$, $P<0.0001$). Upon reoxygenation, T_b recovered very slowly and, after 1 h of reoxygenation, T_b had increased ∼1°C from the lowest hypoxic T_b (28.7±0.04°C) but was still ∼3°C below the pre-treatment normoxic temperature (32.2±0.02°C).

Oxygen consumption rate decreased in progressive hypoxia and was negligible during the early reoxygenation period

NMRs exhibited initial decreases in $\dot{V}_{O_2}$ and $\dot{V}_{CO_2}$ of 55–60% with the onset of hypoxia (9% O_2 inhaled; Fig. 3A,B, left panels; $F_{8,140}=40.88$, $P<0.00001$ for $\dot{V}_{O_2}$, $F_{10,165}=32.08$, $P<0.00001$ for $\dot{V}_{CO_2}$; $n=22$ for each). These changes increased in magnitude with each subsequent level of hypoxia such that the maximum suppression was observed from animals breathing 3% O_2 (87% decrease in $\dot{V}_{O_2}$ and 80% decrease in $\dot{V}_{CO_2}$).

Upon reoxygenation, we found that $\dot{V}_{CO_2}$ dropped further below the maximum suppression observed in 3% O_2 such that $\dot{V}_{CO_2}$ was suppressed by 96 and 90% following 10 and 20 min of reoxygenation, respectively (Fig. 3B, right panel). This apparent metabolic rate suppression decreased progressively through the reoxygenation period and $\dot{V}_{O_2}$ similarly returned slowly to pre-hypoxia baseline levels from 30 min of reoxygenation onward (Fig. 3B, right panel).

Naked mole rats exhibited a fuel switch from mixed lipid/carbohydrate substrate use to pure carbohydrate consumption in acute hypoxia

The NMR RER was 0.74 in normoxia (Fig. 4, left panel; $n=22$), indicating that they predominately use lipid substrates as a metabolic fuel source, with a lesser contribution from carbohydrates. With the onset of progressive hypoxia, NMRs immediately exhibited a shift towards total reliance on carbohydrate substrates ($F_{8,118}=25.00$, $P<0.00001$). Upon reoxygenation, NMRs expressed RER values that were well below 0.7 (Fig. 4, right panel), indicating that the animals were not in steady state; however, their RER values approached pre-hypoxic baseline levels towards the end of the reoxygenation period.

Liver glucose was mobilized in acute hypoxia to support enhanced carbohydrate metabolism but a metabolic acidosis was not observed

To better understand fuel switching following hypoxic exposure, we evaluated metabolic parameters in the blood, brain, heart, temporalis muscle and liver in a subset of NMRs at the end of the progressive hypoxic protocol and compared the resulting values to samples taken from NMRs not exposed to progressive hypoxia (Tables 1, 2). We found that blood glucose levels nearly doubled in acute hypoxia (Table 1), whereas liver glucose levels were markedly lower (Table 2). Together, these observations indicate mobilization of liver glucose stores to support enhanced carbohydrate metabolism when O_2 is low. Glucose levels were not changed in heart, brain or muscle.

Interestingly, we did not observe any signs of a metabolic acidosis in blood or tissues derived from hypoxic animals. Specifically, blood pH was elevated and P_{CO_2} was lower in hypoxic animals, whereas base excess and T_{CO_2} were unchanged with hypoxic treatment (Table 1). Brain pH_i was lower in hypoxic animals but pH_i was not altered in heart, liver or muscle between treatment groups (Table 2).

Importantly, the concentrations of ATP of brain, heart, muscle and liver were not different between normoxic and hypoxic animals (Table 2), indicating that NMRs maintained energy balance during their exposure to progressive hypoxia. However, CrP levels were

Journal of Experimental Biology (2019) 222, jeb191197. doi:10.1242/jeb.191197

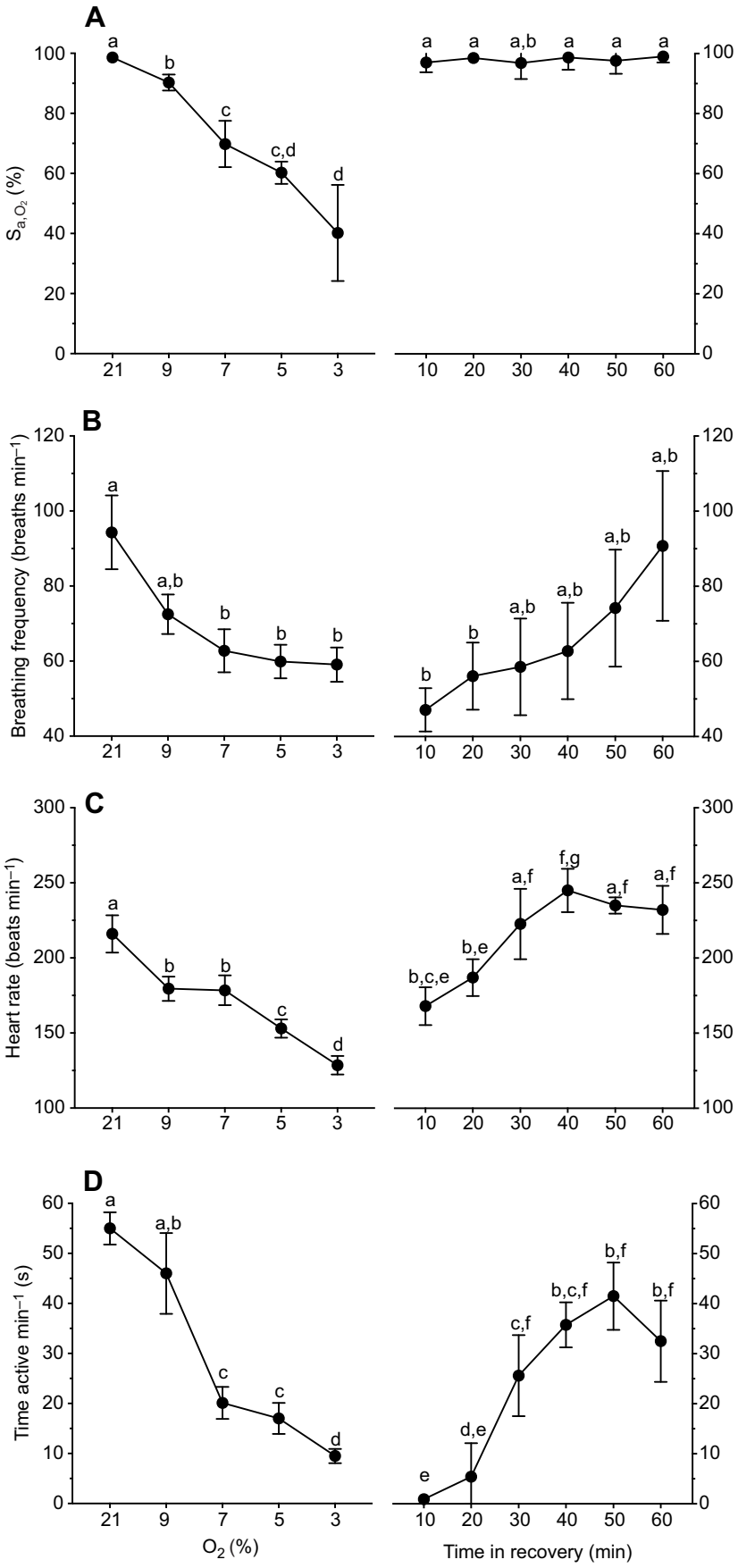

Fig. 1. Naked mole rats (NMRs) exhibit decreases in breathing frequency and heart rate in acute hypoxia that are quickly reversed during reoxygenation. (A–D) Summaries of arterial O_2 saturation (S_{a,O_2}; A; n=8), breathing frequency (B; n=8), heart rate (C; n=22) and behavioural activity (total time active per minute; D; n=8) from NMRs exposed to 21% O_2 and progressive hypoxia (9–3% O_2; 1 h at each; left panels), followed by 1 h of reoxygenation (21% O_2; right panels). Data are presented as means±s.e.m. Significant differences are indicated by different letters. P<0.05.

Journal of Experimental Biology (2019) 222, jeb191197. doi:10.1242/jeb.191197

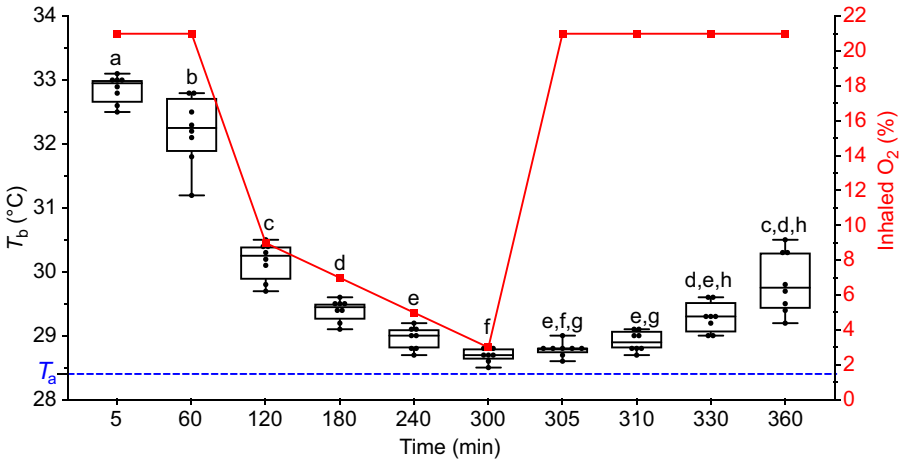

Fig. 2. NMR body temperature (T_b) declines to near ambient temperature (T_a) during acute hypoxia. Summary T_b values from eight NMRs exposed to 21% O_2 and progressive hypoxia (9–3% O_2), followed by 1 h of reoxygenation (21% O_2). T_a is indicated by the dotted line at the bottom of the graph. Inhaled O_2 levels are indicated by the red line and symbols. Box plots indicate 95% confidence intervals with the median represented as the mid-line of each box. Individual replicates for each treatment are indicated by black circles. Data are presented as means±s.e.m. Significant differences are indicated by different letters. P<0.05.

higher in brain and muscle from hypoxic animals, while free adenylate charge was significantly elevated in brain, but not significantly altered in other tissues. Derangements of blood [Na^+], [K^+] and [Ca^{2+}] levels were not observed, indicating that cellular integrity was maintained in the organism (Table 1). Haematocrit and [Hb] measurements were also similar between treatment groups (Table 1).

DISCUSSION

In the present study we examine the hypothesis that NMRs utilize a combined strategy of metabolic rate suppression and upregulation of glycolytic metabolism during acute hypoxic exposure. We predicted that NMRs would exhibit hallmarks of a metabolic acidosis during acute hypoxia and of O_2 debt repayment during the reoxygenation phase following the return to normoxia. We report several significant findings. First, during progressive hypoxia, the oxidative metabolism of NMRs (as measured indirectly through $\dot{V}_{O_2}$ and $\dot{V}_{CO_2}$) is markedly suppressed by as much as 85% of the normoxic rate. This metabolic rate suppression is accompanied by significant reductions in heart rate, f_R, T_b and behavioural activity. During reoxygenation, NMRs enter into a coma-like state lasting 15–20 min, during which they are entirely inactive, are largely non-responsive to external stimuli and exhibit further decreases in their

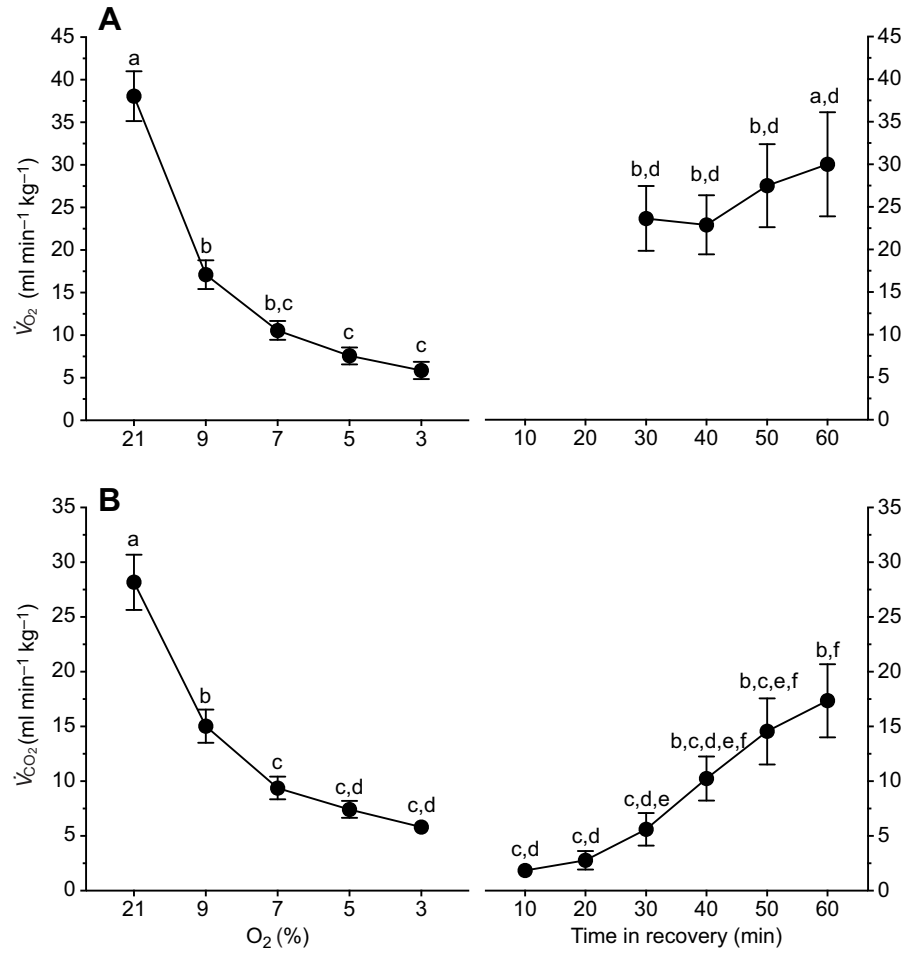

Fig. 3. NMRs exhibit progressively deeper metabolic rate suppression in acute hypoxia, and metabolic rate and behavioural activity are suppressed even further during early reoxygenation. (A,B) Summaries of oxygen consumption rate ($\dot{V}_{O_2}$; A) and carbon dioxide production rate ($\dot{V}_{CO_2}$; B) from 22 NMRs exposed to 21% O_2 and then progressive hypoxia (9–3% O_2; 1 h at each; left panels), followed by 1 h of reoxygenation (21% O_2; right panels). Data are presented as means±s.e.m. Significant differences are indicated by different letters. P<0.05.

Journal of Experimental Biology (2019) 222, jeb191197. doi:10.1242/jeb.191197

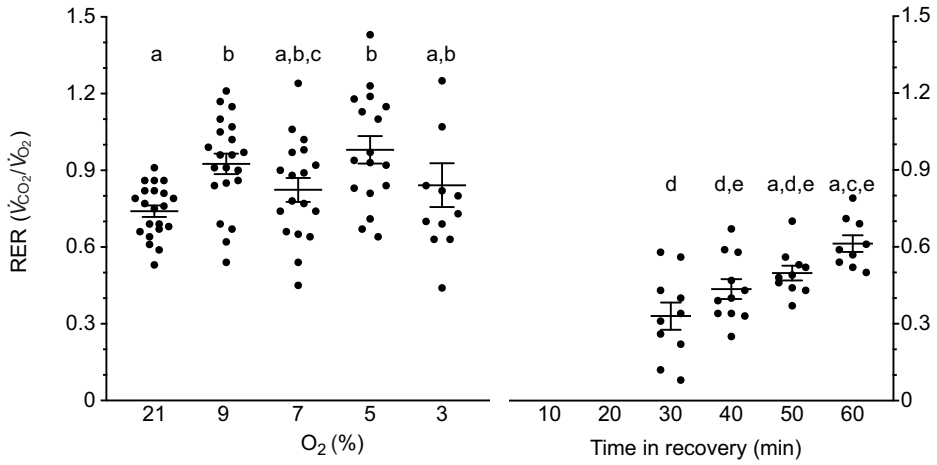

Fig. 4. NMRs exhibit a hypoxic fuel shift, from mixed substrate use (lipids+carbohydrates) to enhanced carbohydrate metabolism, in acute hypoxia. Individual respiratory exchange ratios (RERs; $\dot{V}_{CO_2}/\dot{V}_{O_2}$) from 22 NMRs exposed to 21% O_2 and then progressive hypoxia (9–3% O_2; 1 h at each; left panels), followed by 1 h of reoxygenation (21% O_2; right panels). Data are presented as means±s.e.m. Significant differences are indicated by different letters. P<0.05.

metabolic rate (>95% suppression of $\dot{V}_{CO_2}$). Importantly, at the end of our hypoxic protocol, ATP concentrations in major organs are maintained and adenylate energy charge is sustained or increased in all tissues examined at normoxic levels, indicating that net energy production meets energy demand under hypoxic conditions. In addition, blood and tissue pH levels are largely unchanged after acute hypoxia, suggesting the absence of a metabolic acidosis. Finally, our RER data indicate that NMRs undergo a fuel substrate switch from a reliance on mixed fuel (predominately lipids) in normoxia towards complete reliance on carbohydrates in severe hypoxia. This conclusion is supported by our observations of the mobilization of glucose from the liver into the blood. Taken together, these data indicate that NMRs may not recruit anaerobic metabolic processes or accumulate an O_2 debt during acute hypoxia but may instead rely on substrate modifications to enhance the efficiency of energy production, and thereby support sustained consciousness and activity despite a remarkably deep suppression of metabolic rate.

These data are not unequivocal, however. An imbalance in the rates at which $\dot{V}_{O_2}$ and $\dot{V}_{CO_2}$ return to normoxic levels during reoxygenation hint at the possibility that NMRs do utilize anaerobic metabolism during hypoxia in combination with a tissue and/or blood buffering capacity that masks typical markers of metabolic acidosis, and prioritize the synthesis of glucose from lactate instead of lactate oxidation during recovery. Alternatively, NMRs may rely upon fructose metabolism in hypoxia, as they do in anoxia (Park et al., 2017), to support carbohydrate metabolism without developing a significant lactate accumulation. Finally, several mechanisms related to lactate handling *in vivo* may mitigate the effects of lactate accumulation during hypoxia. For example, changes in the expression of monocarboxylate transporters in anaerobically active tissues or upregulation of gluconeogenesis in the liver may play an important role (Choi et al., 2005); further experiments are warranted to test these possibilities.

Table 1. Blood characteristics from naked mole rats (NMRs) treated in 4 h of normoxia (21% O_2) or progressive hypoxia (9–3% O_2)

Parameter	Normoxia (n=7)	Hypoxia (n=6)
pH	7.43±0.02	7.55±0.26*
P_{CO_2} (mmHg)	29.40±3.69	17.40±1.49*
P_{O_2} (mmHg)	24.67±2.96	25.00±2.40
Base excess	–5.42±2.10	–8.33±1.71
HCO_3^- (mmol l^{-1})	20.83±2.12	15.62±1.70
T_{CO_2}	21.86±2.30	16.33±1.80
Na^+ (mmol l^{-1})	150.29±2.99	142.17±1.38
K^+ (mmol l^{-1})	4.04±0.37	5.23±0.60
$[Ca^{2+}]_i$ (mmol l^{-1})	1.03±0.17	1.40±0.18
Glucose (mg dl^{-1})	86.00±8.38	157.83±38.2*
Hct (%; iSTAT)	34.00±2.53	36.50±2.29
Hct (%; manual)	37.08±1.92	37.13±2.18
Hb (mmol l^{-1}; iSTAT)	11.56±0.86	12.4±0.78
Hb (mmol l^{-1}; Drabkin's assay)	10.60±0.60	9.99±0.47

Data are means±s.e.m. Asterisks indicate significant differences between normoxia and hypoxia (P<0.05).

Naked mole rats reduce behavioural activity and O_2 supply in acute hypoxia and enter into a brief coma-like state during early reoxygenation

NMRs exhibit a unique physiological and behavioural response to acute hypoxia and reoxygenation. Most hypoxia-intolerant adult mammals increase their activity in hypoxia in an attempt to escape to a more hospitable environment, whereas most hypoxia-tolerant vertebrates and small rodents (for the most part) enter into a torpor-like state when O_2 is limited (typically 3–8% O_2; Hayden and Lindberg, 1970). Physiologically, all adult mammals exhibit a hypoxic ventilatory response mediated by increased ventilation, and/or decreased metabolic rate, immediately following hypoxic exposure (Pamenter et al., 2014; Pamenter and Powell, 2016), which is typically accompanied by an increase in heart rate (Dzal et al., 2015). Upon reoxygenation, most animals continue to hyperventilate to blow off CO_2 as part of the repayment of the O_2 debt (i.e. as lactate is oxidised to CO_2+H_2O). Conversely, NMRs exhibit a behavioural pattern that is the inverse of this typical adult mammalian response: they reduce their physical activity in hypoxia but remain responsive to their environment. This behavioural decrease is accompanied by decreases in f_R and heart rate, and also a reduction in T_b to near T_a. These findings agree with previous behavioural and physiological studies from our laboratory (Chung et al., 2016; Houlahan et al., 2018; Ilacqua et al., 2017; Kirby et al., 2018; Pamenter et al., 2015). Upon reoxygenation, NMRs enter into a coma-like state (whereas other mammals emerge from a torpor-like state in this period), during which ventilation is further suppressed but heart rate increases.

Naked mole rats exhibit metabolic depression during hypoxia and do not exhibit an overshoot of metabolic rate during reoxygenation

The decreases in physiological function described above likely all reduce energy demands during hypoxia and support metabolic rate suppression. Indeed, a key finding of our study is that NMRs reduce their metabolic rate by a remarkable 85% in acute severe hypoxia,

Table 2. Tissue metabolic parameters from NMRs treated in 4 h of normoxia or hypoxia (7% O_2)

Parameter	Glucose (μmol l^{-1})	ATP (μmol l^{-1})	CrP (μmol l^{-1})	pH_i	Adenylate charge
Brain					
Normoxia	32.3±5.4	61.1±6.4	268.3±9.2	7.09±0.045	0.96±0.01
Hypoxia	27.7±3.0	53.9±7.1	593.9±107.8*	6.87±0.017*	0.99±0.004*
Heart					
Normoxia	29.7±7.1	124.5±13.5	25.7±8.0	7.13±0.012	0.50±0.14
Hypoxia	21.0±2.6	86.5±24.7	26.8±6.6	7.16±0.037	0.54±0.11
Liver					
Normoxia	995.2±134.9	45.7±7.5	7.7±0.6	7.10±0.016	0.32±0.39
Hypoxia	391.0±159.2*	52.6±7.7	11.5±3.1	7.08±0.058	0.47±0.16
Muscle					
Normoxia	127.4±18.6	315.2±19.6	140.8±20.6	7.22±0.073	0.86±0.05
Hypoxia	151.0±23.7	363.4±22.3	242.8±4.8*	7.16±0.061	0.97±0.004

Data are means±s.e.m. for blood glucose, ATP, creatine phosphate (CrP), intracellular pH (pH_i) and adenylate charge (n=4 for all tissues and variables). Asterisks indicate significant differences between normoxia and hypoxia (P<0.05).

which is very near the threshold at which their energetic demands could be entirely met through anaerobic metabolism (~90–95% suppression) (Mookerjee et al., 2017). However, upon reoxygenation, NMRs do not exhibit an overshoot in their metabolic rate, which is a hallmark of O_2 debt repayment (Coffman, 1963; Lewis et al., 2007; Maxime et al., 2000; Plambech et al., 2013; Svendsen et al., 2012). These findings suggest that they do not rely on anaerobic energy production to a large degree in hypoxia (but see discussion of fructose metabolism, below). In support of this, we do not observe signs of metabolic acidosis in heart, muscle, liver or blood. Specifically, pH values for these samples are not changed by hypoxic exposure, and neither are blood base excess, [HCO_3^-] or T_{CO_2}.

Recently, several groups have proposed that NMRs retain a neonatal phenotype into adulthood and that this neotenic phenotype may contribute to the hypoxia tolerance of this species (Pamenter et al., 2015; Penz et al., 2015; Peterson et al., 2012). However, the fact that NMRs maintain metabolic rate depression for a prolonged period following reoxygenation is in striking contrast to the phenotype of neonatal mammals, in which metabolic rate rapidly returns to normoxic levels (Frappell et al., 1991). Indeed, many neonates exposed to severe hypoxia or to ischemia develop a metabolic acidosis and exhibit the accumulation of an O_2 debt that is then repaid upon reoxygenation (Fahey and Lister, 1989; Frappell et al., 1991). However, the O_2 debt in neonates tends to be less than that observed in adults. Therefore, the neotenic response should be considered as a blunting of the O_2 debt relative to adults, rather than the absence thereof.

Metabolic fuel use during acute hypoxia is indicative of reliance on carbohydrate substrates

Another important finding of our study is the observation that NMRs exhibit a sustained shift of metabolic fuel substrate use from primarily lipids (with some contribution from carbohydrates) in normoxia to a greater reliance on carbohydrates in severe hypoxia. The mobilization of liver glucose stores and increase in blood [glucose] during hypoxic exposure supports an increased reliance on carbohydrate metabolism. This response is similar to that observed in other hypoxia-tolerant rodents, including murine species that live at high altitudes (Schippers et al., 2012). The ATP yield per mole of O_2 catabolized is 15–30% higher when derived from carbohydrates than from lipids (due to the higher energetic costs of breaking high-energy bonds in lipids) and thus a greater reliance on carbohydrate fuels would increase energetic efficiency during acute hypoxia (Hochachka, 1985). The stability seen in our energy charge measurements supports this efficiency, as the metabolic suppression by NMRs may outweigh reductions in ATP production. This strategy would be particularly useful in NMRs because they likely experience hypoxia transiently during intense exercise (e.g. when digging tunnels) and thus would have opportunities to replenish carbohydrate stores while in regions of their burrows with higher levels of O_2, when they rely more heavily on lipid energy stores (as indicated from our normoxic RER calculations). This fuel switch, along with a remarkable metabolic rate depression, may limit the need to recruit anaerobic metabolism and thus the need to pay off O_2 debt post-hypoxia.

NMRs mobilize both glucose and fructose in acute anoxia and are able to metabolize fructose in anoxia (Park et al., 2017); it is possible that fructose contributes to carbohydrate metabolism in severe hypoxia as well. However, the anoxia-induced elevation of glucose in NMRs *in vivo* is considerably greater than that of fructose (Park et al., 2017), and the source of metabolic fructose in NMRs exposed to anoxia is unclear. It is important to note that, although remarkable for a mammal, the ability of NMRs to tolerate a few minutes of anoxia pales in comparison to animals that are truly anoxia tolerant and able to survive in anoxia for days to months (Bickler and Buck, 2007). NMRs should not be considered anoxia tolerant but are more accurately able to resist the lethal effects of anoxia for a short period of time. In this context, it is notable that fructose metabolism also occurs in pathophysiological heart disease in humans (Mirtschink et al., 2015), and it is possible that the ability of NMRs to mobilize and metabolize fructose in acute anoxia reflects a 'last-ditch' effort to survive in such harsh environmental conditions. If this were the case, we would not expect NMRs to mobilize and metabolize fructose while in sublethal levels of hypoxia. Nonetheless, further experiments to assess changes in the fructose transporter Glut5 and liver fructokinase would be fascinating.

It is also important to note that lactate transport strategies may be beneficially modulated during acute hypoxia in this species, but our study does not address this question. Specifically, monocarboxylate transporters are transmembrane proteins that facilitate the transport of lactate across cell membranes. The expression of monocarboxylate transporter 4 in particular is sensitive to hypoxia and is differentially modulated following a day of hypoxia exposure in various tissues in rats and zebrafish (McClelland and Brooks, 2002; Ngan and Wang, 2009; Ullah et al., 2006). Clearance of lactate from NMR tissues that preferentially utilize anaerobic metabolism during hypoxia would support sustained glycolysis and limit the inhibitory effect of accumulated lactate on glycolytic throughput. Studies to date that have examined hypoxia-mediated changes of monocarboxylate transporter expression *in vivo* have largely found that this change follows

several days of hypoxia exposure and not hours. Therefore, it is unlikely that significant insertion of this protein occurs within a few hours of acute hypoxia in NMR tissues. However, higher endogenous expression of these transporters may prime NMR tissues for prolonged anaerobic metabolism.

The conversion of lactate to glucose combined with enhanced buffering capacities may mask the recruitment of anaerobic metabolism in hypoxic NMRs

It is informative to consider lactate management strategies employed by other hypoxia-tolerant vertebrates. In goldfish, which are among the most anoxia-tolerant vertebrates identified and which exhibit marked metabolic rate suppression during periods of anoxia or hypoxia (Vanwaversveld et al., 1989), O_2 debt is not observed following up to 3 h of anoxia but manifests following longer anoxic exposures (Vandenthillart and Verbeek, 1991). In this species, the O_2 debt is hypothesized to be related to the recovery of glycogen pools (Mandic et al., 2008) rather than to the oxidation of lactate because goldfish produce ethanol as an alternative end-product to lactate and thus do not face the same metabolic challenges associated with lactate clearance as do most other vertebrates following exposure to hypoxia (Shoubridge and Hochachka, 1980). Similarly, western painted turtles, which are the most anoxia-tolerant vertebrates, rely entirely on anaerobic metabolism while overwintering in anoxic conditions and accumulate extremely high levels of plasma lactate (Ultsch and Jackson, 1982). However, upon reoxygenation these animals do not exhibit significant lactate oxidation and instead the majority of the accumulated lactate is utilized to restore glycogen pools depleted by the reliance on anaerobic metabolic processes for months (Jackson et al., 1996). Importantly, like NMRs in hypoxia, goldfish and turtles are able to maintain their tissue ATP concentrations during anoxic exposure (Buck and Hochachka, 1993; Mandic et al., 2008), thus reducing the need to regenerate stores of phosphorylated energetic substrates (and thereby the need to ramp up oxidative phosphorylation above pre-anoxic levels during reoxygenation).

Given these strategies of other hypoxia/anoxia-tolerant vertebrates, it is tempting to speculate that NMRs similarly convert lactate accumulated due to anaerobic metabolism in hypoxia to glucose and/or glycogen during hypoxia and also during the reoxygenation phase. Specifically, lactate generated by anaerobic tissues in hypoxia (e.g. muscle, brain, heart) might be transported via the blood to the liver, wherein it could be converted back to glucose via the Cori cycle (Choi et al., 2005; Proia et al., 2016). The resulting glucose would then be available to be transported back to active tissues to sustain further anaerobic metabolism. Importantly, this process is a net consumer of ATP as six molecules of liver ATP are required to convert a molecule of lactate to a molecule of glucose, whereas glucose metabolism by an active tissue only yields two ATP via glycolysis. However, although this conversion yields considerably less net energy than the oxidation of lactate to CO_2 and H_2O, it also confers the distinct advantage of conserving carbon molecules that would otherwise be lost through ventilation. In a nutrient poor environment such as fossorial habitats, the retention of this macromolecule may be a distinct advantage for this species. The sustainment of this process during reoxygenation would explain the lack of an increase in metabolic rate during this stage and might also underlie the nearly comatose behavioural profile of NMRs, as energetic production might be temporarily minimized to support more rapid re-establishment of glucose pools.

Given that we do not observe a metabolic acidosis, NMRs may also express significant buffering capacity in their blood and/tissues to compensate for the H^+ load generated during anaerobic metabolism. In light of this hypothesis, it is notable that the NMR $\dot{V}_{O_2}$ recovers to pre-hypoxia levels far more rapidly than $\dot{V}_{CO_2}$ during reoxygenation; this imbalance may reflect carbon sequestration to re-establish HCO_3^- pools, which are depleted (albeit not significantly so) in the blood of hypoxic animals. In support of this possibility, it is interesting to note that NMRs do not exhibit systemic acidosis when inhaling CO_2 levels <10% (as measured with an abdominal probe in anaesthetized animals) (Park et al., 2017), which suggests that this species may indeed have adaptations to buffer their physiology in environments or conditions that would tend to induce acidosis. Further experiments are warranted to evaluate this hypothesis.

Conclusions

Taken together, these results suggest that either: (1) anaerobic metabolism is not strongly recruited in this species, (2) NMRs utilize anaerobic metabolism and also possess potent buffering capacities in their blood and/or tissues that allow them to focus on replenishing glucose stores during reoxygenation over eliminating accumulated lactate loads, or (3) endogenous priming of lactate clearance mechanisms from cells and upregulation of gluconeogenesis support anaerobic metabolism while minimizing the deleterious consequences of this pathway upon reoxygenation. In any case, the marked reductions in behavioural activity and physiological and thermoregulatory function during acute hypoxia, combined with the switch to fuel substrates that yield more energy per molecule of O_2, minimize the degree to which the animals must rely on anaerobic metabolism. We speculate that these responses are a unique adaptation in this species that enables them to conduct important energetically expensive activities, such as digging new tunnels through dense and hard soils, in severely hypoxic environments.

Acknowledgements

We thank the UBC animal care and veterinary services team for their assistance in animal handling and husbandry.

Competing interests

The authors declare no competing or financial interests.

Author contributions

Conceptualization: M.E.P., Y.A.D., W.K.M.; Methodology: M.E.P., Y.A.D., W.A.T.; Software: Y.A.D., W.K.M.; Validation: M.E.P., Y.A.D.; Formal analysis: M.E.P., Y.A.D., W.A.T.; Investigation: M.E.P., Y.A.D.; Resources: M.E.P., W.K.M.; Data curation: M.E.P., Y.A.D.; Writing - original draft: M.E.P.; Writing - review & editing: M.E.P., Y.A.D., W.A.T., W.K.M.; Visualization: M.E.P.; Supervision: W.K.M.; Project administration: M.E.P., W.K.M.; Funding acquisition: W.K.M.

Funding

This work was supported by a Natural Sciences and Engineering Research Council of Canada (NSERC) Discovery grant to W.K.M., and a Parker B. Francis Foundation Fellowship to M.E.P.

References

Atkinson, D. E. (1968). Energy charge of the adenylate pool as a regulatory parameter. Interaction with feedback modifiers. *Biochemistry* **7**, 4030-4034.

Bates, D., Machler, M., Bolker, B. M. and Walker, S. C. (2015). Fitting linear mixed-effects models using lme4. *J. Stat. Softw.* **67**, 1-48.

Bergmeyer, H. U. (1965). *Methods of Enzymatic Analysis*. New York: Academic Press.

Bickler, P. E. and Buck, L. T. (2007). Hypoxia tolerance in reptiles, amphibians, and fishes: life with variable oxygen availability. *Annu. Rev. Physiol.* **69**, 145-170.

Buck, L. T. and Hochachka, P. W. (1993). Anoxic suppression of Na(+)-K(+)-ATPase and constant membrane potential in hepatocytes: support for channel arrest. *Am. J. Physiol.* **265**, R1020-R1025.

Buck, L. T. and Pamenter, M. E. (2006). Adaptive responses of vertebrate neurons to anoxia-Matching supply to demand. *Respir. Physiol. Neurobiol.* **154**, 226-240.

Buck, L. T. and Pamenter, M. E. (2018). The hypoxia-tolerant vertebrate brain: arresting synaptic activity. *Comp. Biochem. Physiol. B Biochem. Mol. Biol.* **224**, 61-70.

Choi, J. H., Park, M. J., Kim, K. W., Choi, Y. H., Park, S. H., An, W. G., Yang, U. S. and Cheong, J. (2005). Molecular mechanism of hypoxia-mediated hepatic gluconeogenesis by transcriptional regulation. *FEBS Lett.* **579**, 2795-2801.
Chung, D., Dzal, Y. A., Seow, A., Milsom, W. K. and Pamenter, M. E. (2016). Naked mole rats exhibit metabolic but not ventilatory plasticity following chronic sustained hypoxia. *Proc. Biol. Sci.* **283**.
Coffman, J. D. (1963). Blood flow and oxygen debt repayment in exercising skeletal muscle. *Am. J. Physiol.* **205**, 365-369.
Dzal, Y. A., Jenkin, S. E., Lague, S. L., Reichert, M. N., York, J. M. and Pamenter, M. E. (2015). Oxygen in demand: how oxygen has shaped vertebrate physiology. *Comp. Biochem. Physiol. A Mol. Integr. Physiol.* **186**, 4-26.
Fahey, J. T. and Lister, G. (1989). Response to low cardiac-output-developmental differences in metabolism during oxygen deficit and recovery in lambs. *Pediatr. Res.* **26**, 180-187.
Frappell, P., Saiki, C. and Mortola, J. P. (1991). Metabolism during normoxia, hypoxia and recovery in the newborn kitten. *Respir. Physiol.* **86**, 115-124.
Golding, E. M., Teague, W. E. and Dobson, G. P. (1995). Adjustment of K' to varying Ph and Pmg for the creatine-kinase, adenylate kinase and Atp hydrolysis equilibria permitting quantitative bioenergetic assessment. *J. Exp. Biol.* **198**, 1775-1782.
Guppy, M. and Withers, P. (1999). Metabolic depression in animals: physiological perspectives and biochemical generalizations. *Biol. Rev. Camb. Philos. Soc.* **74**, 1-40.
Hayden, P. and Lindberg, R. G. (1970). Hypoxia-induced torpor in pocket mice (genus: Perognathus). *Comp. Biochem. Physiol.* **33**, 167-179.
Hochachka, P. W. (1985). Exercise limitations at high altitude: The metabolic problem and search for its solution. In *Circulation, Respiration, and Metabolism* (ed. R. Giles), pp. 240-249. Berline: Springer-Verlag.
Hochachka, P. W. (1986). Defense strategies against hypoxia and hypothermia. *Science* **231**, 234-241.
Hochachka, P. W., Buck, L. T., Doll, C. J. and Land, S. C. (1996). Unifying theory of hypoxia tolerance: molecular/metabolic defense and rescue mechanisms for surviving oxygen lack. *Proc. Natl. Acad. Sci. USA* **93**, 9493-9498.
Holmes, M. M., Goldman, B. D., Goldman, S. L., Seney, M. L. and Forger, N. G. (2009). Neuroendocrinology and sexual differentiation in eusocial mammals. *Front. Neuroendocrinol.* **30**, 519-533.
Houlahan, C. R., Kirby, A. M., Dzal, Y. A., Fairman, G. D. and Pamenter, M. E. (2018). Divergent behavioural responses to acute hypoxia between individuals and groups of naked mole rats. *Comp. Biochem. Physiol. B Biochem. Mol. Biol.* **224**, 38-44.
Ilacqua, A. N., Kirby, A. M. and Pamenter, M. E. (2017). Behavioural responses of naked mole rats to acute hypoxia and anoxia. *Biol. Lett.* **13**.
Jackson, D. C., Toney, V. I. and Okamoto, S. (1996). Lactate distribution and metabolism during and after anoxia in the turtle, Chrysemys picta bellii. *Am. J. Physiol.* **271**, R409-R416.
Kirby, A. M., Fairman, G. and Pamenter, M. E. (2018). Atypical behavioural, metabolic, and thermoregulatory responses to hypoxia in the naked mole rat (*Heterocephalus glaber*). *J. Zool.* (In press) **305**, 106-115.
Lanza, I. R., Wigmore, D. M., Befroy, D. E. and Kent-Braun, J. A. (2006). In vivo ATP production during free-flow and ischaemic muscle contractions in humans. *J. Physiol.* **577**, 353-367.
Lawson, J. W. R. and Veech, R. L. (1979). Effects of Ph and free Mg2+ on the Keq of the creatine-kinase reaction and other phosphate hydrolyses and phosphate transfer-reactions. *J. Biol. Chem.* **254**, 6528-6537.
Lenth, R. V. (2016). Least-squares means: the R Package lsmeans. *J. Stat. Softw.* **69**, 1-33.
Lewis, J. M., Costa, I., Val, A. L., Almeida-Val, V. M. F., Gamperl, A. K. and Driedzic, W. R. (2007). Responses to hypoxia and recovery: repayment of oxygen debt is not associated with compensatory protein synthesis in the Amazonian cichlid, Astronotus ocellatus. *J. Exp. Biol.* **210**, 1935-1943.
Lighton, J. (2008). *Measuring Metabolic Rates: a Manual for Scientists*. Oxford: Oxford University Press.
Mandic, M., Lau, G. Y., Nijjar, M. M. S. and Richards, J. G. (2008). Metabolic recovery in goldfish: a comparison of recovery from severe hypoxia exposure and exhaustive exercise. *Comp. Biochem. Physiol. C Toxicol. Pharmacol.* **148**, 332-338.
Maxime, V., Pichavant, K., Boeuf, G. and Nonnotte, G. (2000). Effects of hypoxia on respiratory physiology of turbot, Scophthalmus maximus. *Fish Physiol. Biochem.* **22**, 51-59.
McClelland, G. B. and Brooks, G. A. (2002). Changes in MCT 1, MCT 4, and LDH expression are tissue specific in rats after long-term hypobaric hypoxia. *J. Appl. Physiol.* **92**, 1573-1584.
Mirtschink, P., Krishnan, J., Grimm, F., Sarre, A., Horl, M., Kayikci, M., Fankhauser, N., Christinat, Y., Cortijo, C., Feehan, O. et al. (2015). HIF-driven SF3B1 induces KHK-C to enforce fructolysis and heart disease. *Nature* **522**, 444-449.
Mookerjee, S. A., Gerencser, A. A., Nicholls, D. G. and Brand, M. D. (2017). Quantifying intracellular rates of glycolytic and oxidative ATP production and consumption using extracellular flux measurements. *J. Biol. Chem.* **292**, 7189-7207.
Ngan, A. K. and Wang, Y. S. (2009). Tissue-specific transcriptional regulation of monocarboxylate transporters (MCTs) during short-term hypoxia in zebrafish (Danio rerio). *Comp. Biochem. Physiol. B Biochem. Mol. Biol.* **154**, 396-405.
Pamenter, M. E. and Powell, F. L. (2016). Time domains of the hypoxic ventilatory response and their molecular basis. *Comp. Physiol.* **6**, 1345-1385.
Pamenter, M. E., Carr, J. A., Go, A., Fu, Z., Reid, S. G. and Powell, F. L. (2014). Glutamate receptors in the nucleus tractus solitarius contribute to ventilatory acclimatization to hypoxia in rat. *J. Physiol.* **592**, 1839-1856.
Pamenter, M. E., Dzal, Y. A. and Milsom, W. K. (2015). Adenosine receptors mediate the hypoxic ventilatory response but not the hypoxic metabolic response in the naked mole rat during acute hypoxia. *Proc. Biol. Sci.* **282**, 20141722.
Pamenter, M. E., Lau, G. Y., Richards, J. G. and Milsom, W. K. (2018). Naked mole rat brain mitochondria electron transport system flux and H(+) leak are reduced during acute hypoxia. *J. Exp. Biol.* **221**, jeb171397.
Park, T. J., Reznick, J., Peterson, B. L., Blass, G., Omerbasic, D., Bennett, N. C., Kuich, P. H. J. L., Zasada, C., Browe, B. M., Hamann, W. et al. (2017). Fructose-driven glycolysis supports anoxia resistance in the naked mole-rat. *Science* **356**, 305-308.
Penz, O. K., Fuzik, J., Kurek, A. B., Romanov, R., Larson, J., Park, T. J., Harkany, T. and Keimpema, E. (2015). Protracted brain development in a rodent model of extreme longevity. *Sci. Rep.* **5**, 11592.
Peterson, B. L., Park, T. J. and Larson, J. (2012). Adult naked mole-rat brain retains the NMDA receptor subunit GluN2D associated with hypoxia tolerance in neonatal mammals. *Neurosci. Lett.* **506**, 342-345.
Plambech, M., Van Deurs, M., Steffensen, J. F., Tirsgaard, B. and Behrens, J. W. (2013). Excess post-hypoxic oxygen consumption in Atlantic cod Gadus morhua. *J. Fish Biol.* **83**, 396-403.
Portner, H. O., Finke, E. and Lee, P. G. (1996). Metabolic and energy correlates of intracellular pH in progressive fatigue of squid (L-brevis) mantle muscle. *Am. J. Physiol.* **271**, R1403-R1414.
Proia, P., Di Liegro, C. M., Schiera, G., Fricano, A. and Di Liegro, I. (2016). Lactate as a metabolite and a regulator in the central nervous system. *Int. J. Mol. Sci.* **17**, 1450.
Riccio, A. P. and Goldman, B. D. (2000a). Circadian rhythms of body temperature and metabolic rate in naked mole-rats. *Physiol. Behav.* **71**, 15-22.
Riccio, A. P. and Goldman, B. D. (2000b). Circadian rhythms of locomotor activity in naked mole-rats (Heterocephalus glaber). *Physiol. Behav.* **71**, 1-13.
Robin, E. D. (1980). Of men and mitochondria-coping with hypoxic dysoxia-the 1980 Amberson, J. Burns Lecture. *Am. Rev. Respir. Dis.* **122**, 517-531.
Schippers, M. P., Ramirez, O., Arana, M., Pinedo-Bernal, P. and McClelland, G. B. (2012). Increase in carbohydrate utilization in high-altitude Andean mice. *Curr. Biol.* **22**, 2350-2354.
Shoubridge, E. A. and Hochachka, P. W. (1980). Ethanol: novel end product of vertebrate anaerobic metabolism. *Science* **209**, 308-309.
Svendsen, J. C., Steffensen, J. F., Aarestrup, K., Frisk, M., Etzerodt, A. and Jyde, M. (2012). Excess posthypoxic oxygen consumption in rainbow trout (Oncorhynchus mykiss): recovery in normoxia and hypoxia. *Can. J. Zool.* **90**, 1-11.
Teague, W. E., Golding, E. M. and Dobson, G. P. (1996). Adjustment of K' for the creatine kinase, adenylate kinase and ATP hydrolysis equilibria to varying temperature and ionic strength. *J. Exp. Biol.* **199**, 509-512.
Ullah, M. S., Davies, A. J. and Halestrap, A. P. (2006). The plasma membrane lactate transporter MCT4, but not MCT1, is up-regulated by hypoxia through a HIF-1 alpha-dependent mechanism. *J. Biol. Chem.* **281**, 9030-9037.
Ultsch, G. R. and Jackson, D. C. (1982). Long-term submergence at 3°C of the turtle Chrysemys picta bellii in normoxic and severely hypoxic water. III. Effects of changes in ambient PO2 and subsequent air breathing. *J. Exp. Biol.* **97**, 87-99.
Vandenthillart, G. and Verbeek, R. (1991). Anoxia-induced oxygen debt of goldfish (Carassius-Auratus L). *Physiol. Zool.* **64**, 525-540.
Vanwaversveld, J., Addink, A. D. F. and Vandenthillart, G. (1989). Simultaneous direct and indirect calorimetry on normoxic and anoxic goldfish. *J. Exp. Biol.* **142**, 325-335.
Warren, D. E. and Jackson, D. C. (2008). Lactate metabolism in anoxic turtles: an integrative review. *J. Comp. Physiol. B* **178**, 133-148.